Desalination and Water Treatment
www.deswater.com

doi: 10.1080/19443994.2015.1027282

57 (2016) 8894–8903
April

Taylor & Francis
Taylor & Francis Group

Use of HCl-modified bentonite clay for the adsorption of Acid Blue 129 from aqueous solutions

Zia Ullah[a], Sajjad Hussain[b,*], Saima Gul[c], Sabir Khan[d], F.K. Bangash[a]

[a]*Institute of Chemical Sciences, University of Peshawar, Peshawar 25120, Khyber Pakhtunkhwa, Pakistan, Tel. +92 91 9216652; emails: ziaullahsco@hotmail.com (Z. Ullah), fazlullah52@yahoo.com (F.K. Bangash)*
[b]*Department of Chemistry, Sarhad University of Science and Information Technology, Peshawar, Khyber Pakhtunkhwa, Pakistan, Tel. +92 91 3335741828; email: sajjadchemist@yahoo.com*
[c]*Department of Biochemistry, Shaheed Benazir Bhutto Women University, Peshawar, Khyber Pakhtunkhwa, Pakistan, Tel. +92 91 9239157; email: saimachemist@yahoo.com*
[d]*Instituto de Química de Araraquara, Universidade Estadual Paulista, CP 355, Araraquara, SP 14801-970, Brasil, Tel. +55 16 981619591; email: sabir_chemist@yahoo.com*

Received 8 December 2014; Accepted 27 February 2015

ABSTRACT

The adsorption of Acid Blue 129 (AB129) from aqueous solution onto hydrochloric acid-activated montmorillonite clay (HCl-bentonite) was investigated. The activated clay was characterized by scanning electron microscopy, energy dispersive spectroscopy, and Brunauer–Emmett–Teller surface area. Batch adsorption experiments were performed to investigate the effects of pH, contact time, initial dye concentration, and temperature (10, 20, 30, and 40˚C). Acidic conditions was suitable for higher adsorption of AB129, and kinetic studies demonstrate that the process followed a pseudo-second-order model. An activation energy of 23.858 kJ mol^{-1} was obtained for adsorption process. Adsorption data were fitted to Freundlich and Langmuir isotherms and various adsorption parameters have been calculated. Standard enthalpy (ΔH°) and standard entropy (ΔS°) were −44.90 kJ mol^{-1} and −68.44 kJ mol^{-1} K^{-1}, respectively, showing that overall adsorption process was exothermic and is spontaneous in nature with a decrease in the disorder of the system at the dye/adsorbate interface. However, the mechanism of the dye–Bentonite interaction is likely to be very complicated, involving a wide range of sites having different energy considerations. The activated clay was effective toward adsorption of AB129. The results show that activated bentonite clay could be employed as low-cost materials for the removal of acid dyes from colored effluents.

Keywords: Adsorption; Acid Blue 129; Bentonite clay; Thermodynamics; Kinetics

1. Introduction

There are more than 100,000 types of commercial dyes, with an estimated production of 7×10^5 to 1×10^6 tons per year worldwide [1]. The classification of the dyes is based on their application and chemical structure. Dyes are composed of atoms responsible for the dye color called chromophores as well as an electron-withdrawing or electron-donating substituent that causes or intensifies the color of chromophores, called auxochrome [2,3]. Based on the chemical structure of the chromophores groups, dyes are classified as azo

---

*Corresponding author.

dyes, anthraquinone, triphenylmethane, heterocyclic and polymeric dyes [4]. In textile industries, up to 50% of the dyes are lost in the dyeing process and about 10–15% of the effluents are discarded [5]. The release of textile effluents in the receiving water bodies causes considerable environmental degradation by modifying the natural color and forming foam on its surface [6]. These dyes are invariably left as the major waste in these industries. Due to their chemical structures, dyes are resistant to fading on exposure to light, water, and many chemicals; therefore, these are difficult to be decolorized once released into the environment [7]. Many of the organic dyes are hazardous and may affect aquatic life and even the food chain [8]. The release of dyes into water streams is esthetically undesirable and has serious environmental impacts. Due to intense color, they reduce sunlight transmission into water, hence affecting aquatic plants, which ultimately disturb aquatic ecosystem; in addition, they are toxic to humans also [6,9]. Acid dyes are the most problematic due to their bright color, acidic nature, and water-soluble characteristics. Several studies have been executed on the adsorption of dyes by clay minerals and other bio and agricultural wastes as adsorbents [10–20].

In recent decades, various methods have been developed for the removal of dyes from wastewaters, such as chemical oxidation, biodegradation, membrane separation, electrochemical processes, coagulation/flocculation [21–27], and adsorption [28–38]. Adsorption is considered an effective way to remove dyes from wastewater, since it is a non-destructive, simple, and economical method of treatment [39–45]. The use of activated carbon as an adsorbent has a long history and it has been widely utilized for dye removal in wastewaters. However, due to its high cost, researchers have been studying for alternative adsorbents [46,47]. The present work aims to study the effectiveness of HCl-activated Bentonite to remove Acid Blue 129 (AB129) by the adsorption process. The effect of different adsorption factors such as solution pH, initial dye concentration, contact time, and temperature was studied. The rate constants and activation energy are used to calculate the kinetics of adsorption. Langmuir and Freundlich adsorption isotherms are applied to the experimental data in order to determine the equilibrium and mechanism of the adsorption process.

2. Materials and methods

2.1. Preparation and activation of bentonite clay

The montmorillonite clay (bentonite) was collected from Aza Khel Peshawar, Pakistan. The raw clay was first ground to powder and sieved through a 200-μm sieve. 50 g of refined clay was activated by treating with a reflux of 250 mL of 1 mol L^{-1} HCl solution in a round bottom flask for 2 h at 80°C. The slurry was air cooled, washed with doubly distilled water, and filtered. The filtrate was then dried at 120°C and store in a desiccator for further study.

2.2. Materials and solution

AB129 was purchased from Sigma–Aldrich (Lahore, Pakistan) and applied without further purification. The chemical structure is shown in Fig. 1. The AB129 has molecular formula $C_{23}H_{21}N_2NaO_5S$ with a molar mass of 460.48 g mol^{-1}. Its electronic spectrum has a maximum absorbance peak in the visible region at a wavelength of 629 nm. The stock solution of concentration 1×10^{-3} M was prepared in doubly distilled water. The standard working solutions $1–6 \times 10^{-5}$ M of AB129 were prepared by dilution and all reagents used were of analytical grade.

2.3. Material characterization

Surface morphology was investigated by using scanning electron microscope (SEM), model JSM 5910, JEOL-JAPAN. The chemical composition of the clay was obtained by using energy dispersive X-ray analyzer INCA-200, Oxford instruments, UK. The surface area of the adsorbent was determined by Brunauer–Emmett–Teller (BET)-N_2 adsorption method using Surface Area Analyzer NOVA 2200e Quanta Chrome, USA. Prior to the measurements, the clay samples were degassed at 373 K for 2 h, and then nitrogen adsorption and desorption were measured.

2.4. Adsorption experiments

Adsorption studies were carried out by batch process in a thermostat shaker. 30 mL of 1×10^{-5} to 6×10^{-5} M AB129 was taken in reagent bottles containing 0.1 g of activated clay. The reagent bottles

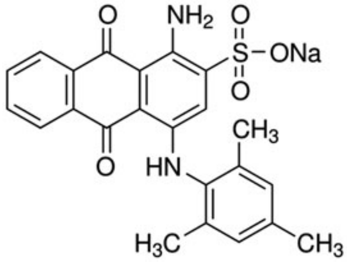

Fig. 1. Chemical structure of dye AB129.

were shaken in a thermostat water bath shaker at 120 rpm. After different time intervals (5–55 min), the samples were taken and then filtered by Whatman filter paper No. 3. The equilibrium concentration of the AB129 was measured through a UV–Visible spectrophotometer (Shimadzu UV-160 A) at $\lambda_{\max}$ 629 nm and the amount of dye adsorbed onto clay surface (q_e, mol g^{-1}) was calculated accordingly [17].

3. Results and discussion

3.1. Material characterization

SEM observations of the activated clay (Fig. 2(a)), reveal rough and irregular surface of the adsorbent that provides large surface area and porosity for adsorption. However, the SEM of the untreated clay (Fig. 2(b)) demonstrated small porosity and small irregularity on the surface, which decline dye adsorption. This conclusion has been proved by the BET surface area measurements, which show that the surface area of the activated clay is 86.65 $m^2 g^{-1}$ and the raw clay is 94.70 $m^2 g^{-1}$, similarly the Langmuir surface area is 929.64 and 1638.66 $m^2 g^{-1}$ for raw and HCl-bentonite, respectively. Energy dispersive spectroscopy (EDS) was also used to analyze elemental composition of raw and HCl-bentonite. It was found that oxygen, silicon, and aluminum were the major consistent components in both clays. Other minor constituents that were obtained from the analyses included magnesium, calcium, and iron. The EDS spectrums are shown in Fig. 3(a) and (b) for raw and HCl-bentonite, respectively.

3.2. Effect of initial solution pH on the adsorption of AB129

pH is an important controlling parameter in any adsorption process and a series of preliminary experiments were performed using pHs varying from 2 to

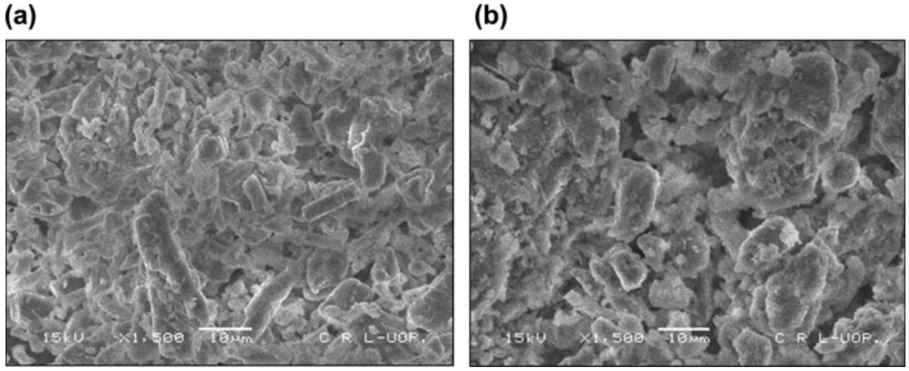

Fig. 2. SEM images of (a) raw bentonite (b) HCl-bentonite sample.

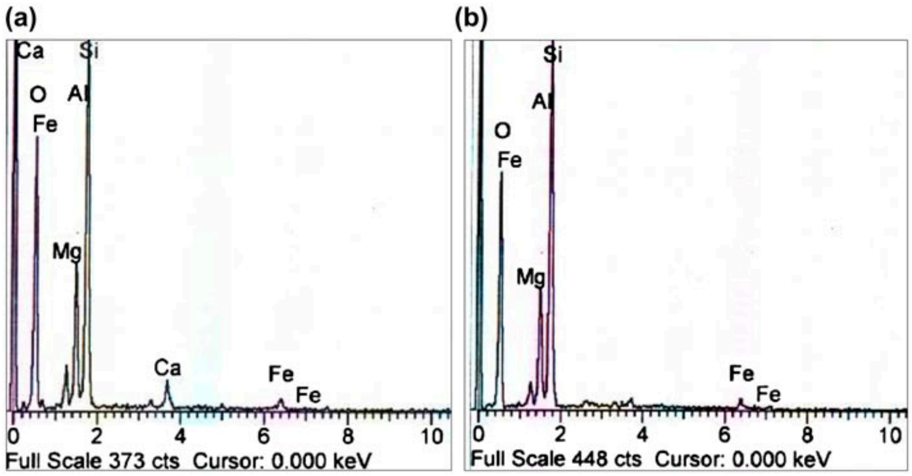

Fig. 3. EDS spectrum of (a) untreated clay and (b) HCl-bentonite.

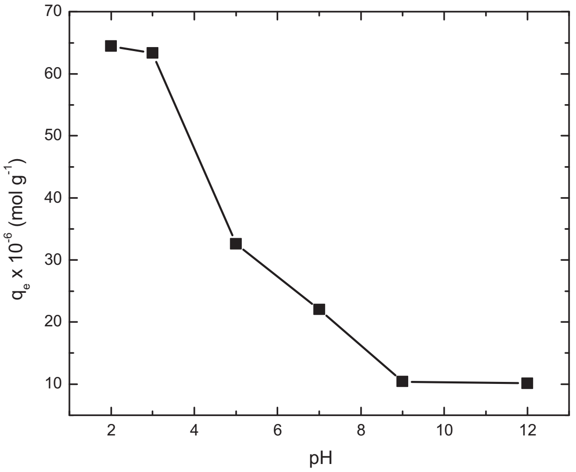

Fig. 4. pH effect on the adsorption of AB129 onto HCl-bentonite (Conditions: $C_{AB129} = 4 \times 10^{-5}$ M, 0.1 g of adsorbent).

12. Fig. 4 represents that the adsorption of AB129 decreased with increasing pH and maximum adsorption occurred between pH 2 and 3. Under acidic conditions, a strong electrostatic attraction exists between the positively charged surface of the clay and acid (anionic) dye. As the pH of the system increases, the number of negatively charged sites increases and the number of positively charged sites decreases, and hence there is a decrease in adsorption. It was observed that the adsorption is highly dependent on the pH of the solution, as reported elsewhere [14,15].

3.3. Comparison of adsorption capacity of raw and HCl-bentonite

Initially, some experiments at pH 3 were conducted in order to investigate the adsorption capacity of both (raw and treated clay). It is obvious from Fig. 5 of that HCl-activated bentonite has a suitable adsorption capacity for the removal of AB129 from aqueous solution than raw bentonite mainly because of the highly porous surface of HCl-bentonite. The natural bentonite is not a highly effective adsorbent for the removal of hydrophobic organic compounds from aqueous solution; this is due to the electrically charged and hydrophilic characteristics of the surface. However, natural bentonite may be modified with acid that significantly improves its capability of removing hydrophobic contaminants from water [14].

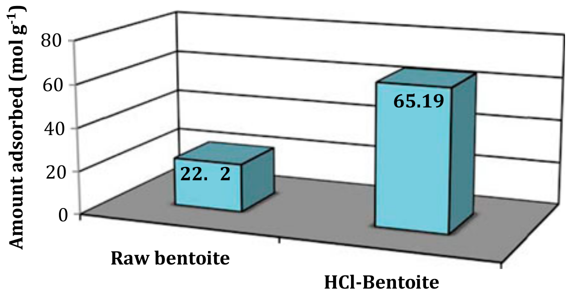

Fig. 5. Comparison of the adsorption capacity of raw bentonite and HCl-bentonite at pH 3.

3.4. Effect of contact time and temperature

The effect of contact time on the adsorption of AB129 at different temperatures was studied. As shown in Fig. 6, adsorption increased with time, and was rapid in the initial 20 min and then continued to increase gradually. 55 min was taken as the equilibrium time. Initially, a large number of active sites are expected to be available on the surface of HCl-bentonite. As the adsorption progresses, the sites become saturated and the rate of adsorption decreases and gets covered, and there is no free space available to the adsorbate molecules. The initial rapid uptake of (up to 20 min) AB129 from solution was likely due to extracellular binding and the slow sorption phase likely resulting from intracellular binding. Due to the high surface area, HCl-bentonite clay shows maximum adsorption for this dye. Fig. 6 also shows the influence of temperature on adsorption; as the temperature increases from 10 to 40℃, the amount of adsorption decreases from 7 to 4.2 mol g^{-1}.

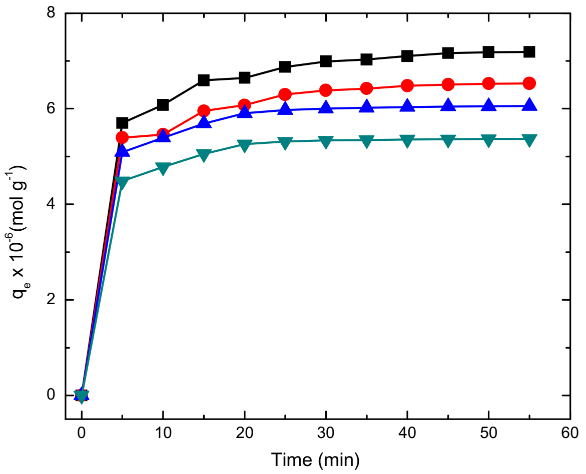

Fig. 6. Effect of contact time on the adsorption of AB129 onto HCl-bentonite at different temperatures (■) 10℃ (●) 20℃ (▲) 30℃ (▼) 40℃ (Conditions: pH_i 3, $C_{AB129} = 4 \times 10^{-5}$ M).

3.5. Adsorption kinetics

In order to investigate the kinetics of adsorption of Acid Blue 129 onto HCl-bentonite clay, pseudo-first-order and pseudo-second-order equations [48,49] were applied. The pseudo-first-order expression is given by following equation:

$$\log(q_e - q_t) = \log q_e - \frac{k_1 t}{2.303} \tag{1}$$

where q_e and q_t are the amounts of AB129 (mol g^{-1}) adsorbed at equilibrium and at time t, respectively. k_1 is the overall rate constant. Straight lines were obtained by plotting $\log(q_e - q_t)$ against t, as shown in Fig. 7. The values of rate constant k_1 were calculated from the slopes of straight lines of Fig. 7 and the values are reported in Table 1. The regression coefficients (R^2) and rate constants at various temperatures are given in Table 1. The pseudo-second-order kinetics model is given in following equation.

$$\frac{t}{q_t} = \frac{1}{k_2\, q_e^2} + \frac{1}{q_e}\, t \tag{2}$$

where q_e is the maximum adsorption capacity (mol g^{-1}) for the pseudo-second-order adsorption, q_t the amount of the dye adsorbed at time t (mol g^{-1}), and k_2 is the equilibrium rate constant of pseudo-second-order adsorption (dm^3 mol^{-1} min^{-1}). The values of k_2 and q_2 were calculated from the plot of t/q_t against t (Fig. 8). The calculated q_e values agree with experimental q_e values, and, also, the correlation coefficients (R^2) for the pseudo-second-order kinetic plots at all the studied concentrations were above 0.9998 (Table 1). These results imply that the adsorption system studied obeys the pseudo-second-order kinetic model. The activation energy E_a for adsorption was found using arrhenius Eq. (3):

$$\ln k_2 = -\frac{E_a}{RT} + \text{constant} \tag{3}$$

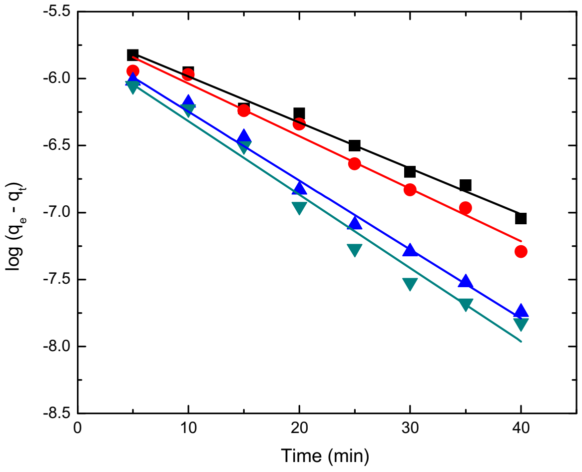

Fig. 7. Pseudo-first-order kinetics of adsorption of AB129 onto HCl-bentonite at different temperatures (■) 10°C (●) 20°C (▲) 30°C (▼) 40°C (Conditions: pH$_i$ 3, $C_{AB129} = 4 \times 10^{-5}$ M).

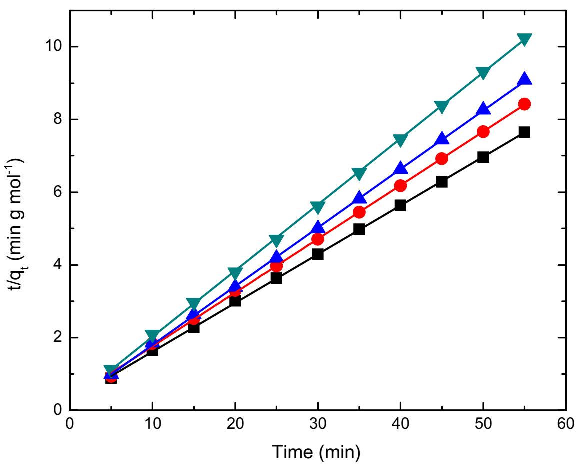

Fig. 8. Pseudo-second-order kinetics of adsorption of AB129 onto HCl-bentonite at different temperatures (■) 10°C (●) 20°C (▲) 30°C (▼) 40°C (Conditions: pH$_i$ 3, $C_{AB129} = 4 \times 10^{-5}$ M).

Table 1
Pseudo-first-order and pseudo-second-order rate constant for adsorption of AB129 onto HCl-bentonite at different temperatures

Pseudo-first-order				Pseudo-second-order			
T (°C)	q_e (mol g^{-1})	k_1 (min^{-1})	R^2	q_e (mol g^{-1})	k_2 (dm^3 mol^{-1} min^{-1})	h (mol g^{-1} min^{-1})	R^2
10	7.19	0.08	0.9890	7.46	0.066	3.66	0.9997
20	6.53	0.09	0.9805	6.77	0.08	3.52	0.9996
30	6.05	0.12	0.9922	6.20	0.14	5.34	0.9998
40	5.37	0.12	0.9778	5.50	0.16	4.82	0.9998

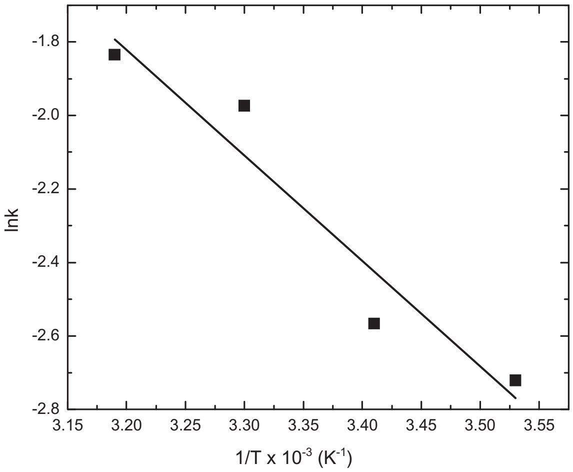

Fig. 9. Arrhenius plot for adsorption of AB129 onto HCl-bentonite.

where E_a is the energy of activation, R is the gas constant, and T is the absolute temperature. Activation energy determined from the slope of the Arrhenius plot of Fig. 9 and was found to be 23.858 kJ mol^{-1}. The physisorption processes usually have energies in the range of 5–40 kJ mol^{-1}, while higher values (40–800 kJ mol^{-1}) suggest chemisorption. The activation energy (23.8587 kJ mol^{-1}) shows that the adsorption of AB129 onto HCl-bentonite clay was mainly physisorption.

3.6. Effect of initial AB129 concentration and adsorption isotherms

In order to clarify the adsorption process, the Freundlich and Langmuir isotherm models were applied to the adsorption of AB129. Experiments were conducted at a fixed adsorbent dosage of 0.1 g and pH 3 at different initial concentrations. Fig. 10 indicates that adsorption increases as the dye concentration increases, which was mainly due to the availability of a large number of sites over the clay surface. Fig. 10 also shows the effect of temperature on the adsorption of AB129 ions from aqueous solution. It is obvious that the amount of dye adsorbed decreases with a rise in temperature, which indicates that the adsorption from aqueous solution onto activated clay is an exothermic process, and this fact explains the diminution of adsorption with the increase in temperature. The reason may be due to the weakening of the attractive forces between the dye and adsorbent sites.

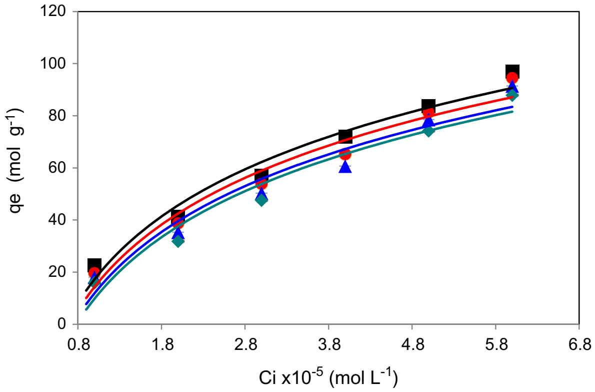

Fig. 10. Effect of AB129 initial concentration on adsorption at different temperatures (■) 10°C (●) 20°C (▲) 30°C (◆) 40°C.

Since the determination of the adsorption isotherm is important in designing the nature of the adsorption system, two isotherm equations have been applied. The data are evaluated by applying the Langmuir and Freundlich isotherms. The linear form of the Langmuir Eq. (4) was applied to the experimental data:

$$\frac{C_e}{q_e} = \frac{1}{K_1 X_m} + \frac{C_e}{X_m} \tag{4}$$

where C_e is the equilibrium concentration (M), q_e is the amount (mol g^{-1}) of AB129 adsorbed; X_m and K_1 are Langmuir constants representing the adsorption capacity (mol g^{-1}) and energy of adsorption (mol g^{-1}), respectively. The linear plot of C_e/q_e versus C_e (Fig. 11) indicates the applicability of Langmuir adsorption isotherm, consequently the formation of

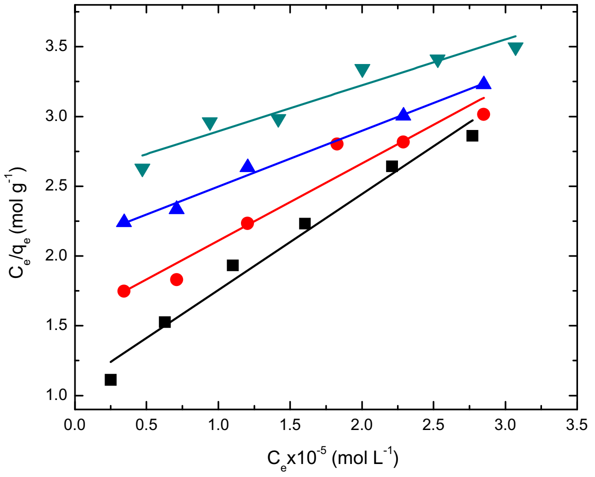

Fig. 11. Langmuir adsorption isotherm for adsorption of AB129 onto HCl-bentonite at different temperatures (■) 10°C (●) 20°C (▲) 30°C (◆) 40°C.

Table 2
Langmuir and Freundlich constants for adsorption of AB129 at different temperatures

	Langmuir constant				Freundlich constant		
T (˚C)	X_{m1} ($\times 10^{-5}$ mol g^{-1})	K_1 ($\times 10^{-4}$ mol L^{-1})	R_L	R^2	$1/n$ (g L^{-1})	K ($\times 10^{-6}$ mol g^{-1})	R^2
10	1.59	6.21	0.64	0.9728	0.54	1.40	0.9979
20	1.01	6.27	0.49	0.9301	0.58	1.48	0.9853
30	2.60	1.78	0.34	0.9898	0.60	1.30	0.9884
40	3.26	1.16	0.08	0.9142	0.63	1.14	0.9949

monolayer on the surface of the adsorbent. Langmuir constant X_m (adsorption capacity) and K_1 (binding energy constant) were calculated from the slopes and intercepts of plots and are given in Table 2.

The Freundlich isotherm is an empirical equation employed to describe the heterogeneous system. The linear form of the Freundlich isotherm was also applied to the adsorption of AB129:

$$\ln\frac{x}{m} = \ln K + \frac{1}{n}\ln C_e \tag{5}$$

where K (mol g^{-1}) and $1/n$ (g L^{-1}) are Freundlich constants, indicating the adsorption capacity and adsorption intensity, respectively. Straight lines were obtained by plotting ln x/m against ln C_e, and K and $1/n$ were calculated from the slope and intercept of these lines (Fig. 12). The values of Freundlich constants are given in Table 2. Since the values of $1/n$ are increases as the temperature increased which indicates favorable adsorption and relatively strong interaction between adsorbate/adsorbent. The values of $1/n$ indicate the formation of a relatively strong bond between adsorbate and adsorbent as temperature rises. For a favorable adsorption, the value of $1/n$ is smaller than 1 and when the unfavorable adsorption takes place, the adsorption bond becomes weak and the value of $1/n$ is greater than 1; so adsorption decreases. As shown in Table 2, the value of $1/n$ for AB129 ions adsorption is less than unity, which shows high adsorption intensity. As the temperature rises from 10 to 40˚C, there is a slight increase in $1/n$ values, which means the adsorption of AB129 is exothermic in nature, which decreases with an increase in temperature. When the values of K and $1/n$ (Table 2) were compared at all the temperatures under study, the results show that higher values of $1/n$ and lower values of K were obtained at higher temperatures. The correlation coefficient is more close to 1 for the Freundlich isotherm that indicates a good agreement with experimental data and isotherm parameters.

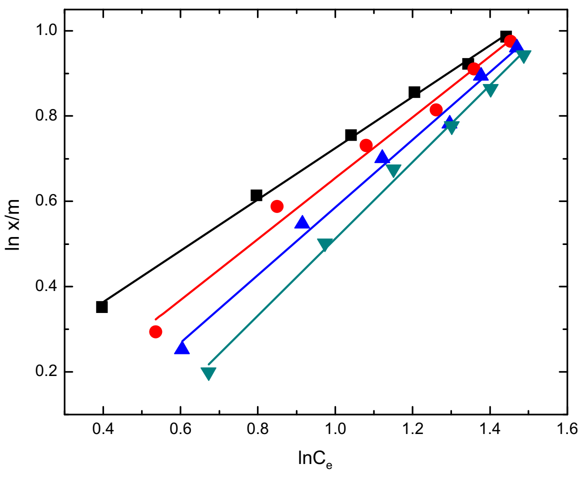

Fig. 12. Freundlich adsorption isotherm for adsorption of AB129 onto HCl-bentonite at different temperatures (■) 10˚C (●) 20˚C (▲) 30˚C (◆) 40˚C.

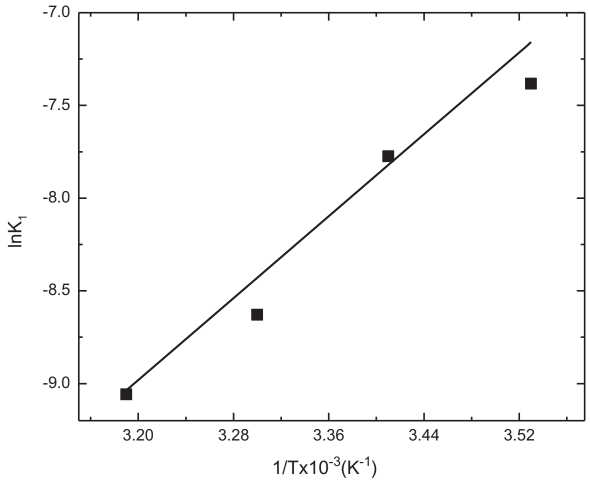

Fig. 13. Plot of lnK_1 vs. $1/T$ for estimation of thermodynamic parameters for the adsorption of AB129 onto HCl-bentonite.

Table 3
Thermodynamic parameters for adsorption of AB129 at different temperatures

T (°C)	$1/T \times 10^{-3}$ (K^{-1})	ln K_1	ΔH (kJ mol^{-1})	ΔS (kJ mol^{-1} K^{-1})	ΔG (kJ mol^{-1})	R^2
10	3.53	1.82	−45.90	−68.44	−25.96	0.9159
20	3.41	1.83			−26.90	
30	3.30	0.58			−24.66	
40	3.19	0.15			−24.36	

3.7. Thermodynamics of adsorption

Various thermodynamic parameters such as ΔG°, ΔS°, and ΔH° of AB129 adsorption were calculated from the binding constant K_1 using the following relations.

$$\Delta G^\circ = -RT \ln K_1 \tag{6}$$

$$\ln K_1 = -\frac{\Delta H^\circ}{RT} + \frac{\Delta S^\circ}{R} \tag{7}$$

The values of ΔH° and ΔS° were calculated from the slope and intercept, respectively, of linear variation of ln K_1 vs. $1/T$ (Fig. 13). The values of ΔG° were calculated using equation 3.6. The values of ΔS°, ΔG°, and ΔH° are given in Table 3. The negative values of ΔG° represent the spontaneous nature of adsorption and indicate the driving force for the affinity of dye toward clay at different temperatures. The ΔG° values are nearly constant, showing that there is no effect of temperature on the free energy of adsorption. Generally, ΔG° for physisorption is between −20 and 0 kJ mol^{-1}, but for chemisorption is in the range of −80 to −400 kJ/mol. As the ΔG° values are nearer to the physisorption range, the adsorption of AB129 onto the HCl-bentonite clay may be physical in nature. However, the mechanism of the dye HCl-bentonite interaction is thus likely to be very complicated, involving a wide range of sites having difference in energies. The negative value of ΔH° shows the process of adsorption is exothermic in nature with the dye removal capacity decreasing with an increase in temperature due to increasing mobility of the dye molecules or it might indicate the operation of weaker attractive forces at higher temperatures. The value of ΔS° is also negative. This is due to the decreased randomness at the solid solution interface and no significant changes occur in the internal structure of the adsorbent through the adsorption of the dye molecules onto clay surface.

4. Conclusions

The modified bentonite clay proved to be an effective adsorbent for the removal of AB129 from aqueous solution, and therefore can be used as a suitable adsorbent for both drinking as well as wastewater treatment. The adsorption process is mainly pH dependent and it was concluded that acidic condition is favorable for the removal of AB129 from the surface of HCl-bentonite. The adsorption process obeys the pseudo-second-order rate equation. The Langmuir and Freundlich models were well fitted to experimental data. The change of equilibrium constant with temperature was used to evaluate various thermodynamic constants. The negative values of ΔG° show that the adsorption process is spontaneous in nature. The values of ΔS° indicate that there is a decrease in the disorderliness of the system, while the negative value of ΔH° proves the process to be exothermic.

Acknowledgments

The authors appreciate the cooperation of lab technicians for the characterization of clay samples at Centralized Recourse Laboratory University of Peshawar, Pakistan.

References

[1] Y. He, J.-F. Gao, F.-Q. Feng, C. Liu, Y.-Z. Peng, S.-Y. Wang, The comparative study on the rapid decolorization of azo, anthraquinone and triphenylmethane dyes by zero-valent iron, Chem. Eng. J. 179 (2012) 8–18.
[2] R. Christie, Colour Chemistry, first ed., The Royal Society of Chemistry, Cambridge, 2001.
[3] A.B. dos Santos, F.J. Cervantes, J.B. van Lier, Review paper on current technologies for decolourisation of textile wastewaters: Perspectives for anaerobic biotechnology, Bioresour. Technol. 98 (2007) 2369–2385.
[4] X.Q. Yang, X.X. Zhao, C.Y. Liu, Y. Zheng, S.J. Qian, Decolorization of azo, triphenylmethane and anthraquinone dyes by a newly isolated *Trametes* sp. SQ01 and its laccase, Process Biochem. 44 (2009) 1185–1189.

[5] W.S. Pereira, R.S. Freire, Azo dye degradation by recycled waste zero-valent iron powder, J. Braz. Chem. Soc. 17 (2006) 832–838.

[6] S. Khan, M. Abdul, Environmental and health effects of textile industry wastewater, in: A. Malik, E. Grohmann, R. Akhtar (Eds.), Environmental Deterioration and Human Health, Springer, Dordrecht, 2014, pp. 55–71.

[7] P. Senthil Kumar, S. Ramalingam, C. Senthamarai, M. Niranjanaa, P. Vijayalakshmi, S. Sivanesan, Adsorption of dye from aqueous solution by cashew nut shell: Studies on equilibrium isotherm, kinetics and thermodynamics of interactions, Desalination 261 (2010) 52–60.

[8] S. Afaq, K. Rana, Toxicological effects of leather dyes on total leukocyte count of fresh water teleost, *Cirrhinus mrigala* (Ham), Biol. Med. 1 (2009) 134–138.

[9] I.A. Aguayo-Villarreal, V. Hernández-Montoya, N.A. Rangel-Vázquez, M.A. Montes-Morán, Determination of QSAR properties of textile dyes and their adsorption on novel carbonaceous adsorbents, J. Mol. Liq. 196 (2014) 326–333.

[10] M.S.U. Rehman, M. Munir, M. Ashfaq, N. Rashid, M.F. Nazar, M. Danish, J.-I. Han, Adsorption of Brilliant Green dye from aqueous solution onto red clay, Chem. Eng. J. 228 (2013) 54–62.

[11] D. Sun, X. Zhang, Y. Wu, T. Liu, Kinetic mechanism of competitive adsorption of disperse dye and anionic dye on fly ash, Int. J. Environ. Sci. Technol. 10 (2012) 799–808.

[12] I.K. Chandra, Y.-H. Ju, A. Ayucitra, S. Ismadji, Evans blue removal from wastewater by rarasaponin–bentonite, Int. J. Environ. Sci. Technol. 10 (2012) 359–370.

[13] L. Cottet, C.A.P. Almeida, N. Naidek, M.F. Viante, M.C. Lopes, N.A. Debacher, Adsorption characteristics of montmorillonite clay modified with iron oxide with respect to methylene blue in aqueous media, Appl. Clay Sci. 95 (2014) 25–31.

[14] A.S. Ozcan, A. Ozcan, Adsorption of acid dyes from aqueous solutions onto acid-activated bentonite, J. Colloid Interface Sci. 276 (2004) 39–46.

[15] A.S. Özcan, B. Erdem, A. Özcan, Adsorption of Acid Blue 193 from aqueous solutions onto BTMA-bentonite, Colloids Surf. A 266 (2005) 73–81.

[16] S. Sadaf, H.N. Bhatti, S. Nausheen, S. Noreen, Potential use of low-cost lignocellulosic waste for the removal of direct violet 51 from aqueous solution: Equilibrium and breakthrough studies, Arch. Environ. Contam. Toxicol. 66 (2014) 557–571.

[17] S. Nawaz, H.N. Bhatti, T.H. Bokhari, S. Sadaf, Removal of Novacron Golden Yellow dye from aqueous solutions by low-cost agricultural waste: Batch and fixed bed study, Chem. Ecol. 30 (2013) 52–65.

[18] S. Noreen, H.N. Bhatti, S. Nausheen, S. Sadaf, M. Ashfaq, Batch and fixed bed adsorption study for the removal of Drimarine Black CL-B dye from aqueous solution using a lignocellulosic waste: A cost affective adsorbent, Ind. Crops Prod. 50 (2013) 568–579.

[19] S. Sadaf, H.N. Bhatti, Batch and fixed bed column studies for the removal of Indosol Yellow BG dye by peanut husk, J. Taiwan Inst. Chem. Eng. 45 (2014) 541–553.

[20] S. Sadaf, H.N. Bhatti, Evaluation of peanut husk as a novel, low cost biosorbent for the removal of Indosol Orange RSN dye from aqueous solutions: Batch and fixed bed studies, Clean Technol. Environ. Policy 16 (2013) 527–544.

[21] K. Dutta, S. Mukhopadhyay, S. Bhattacharjee, B. Chaudhuri, Chemical oxidation of methylene blue using a Fenton-like reaction, J. Hazard. Mater. 84 (2001) 57–71.

[22] E. Castro, A. Avellaneda, P. Marco, Combination of advanced oxidation processes and biological treatment for the removal of benzidine-derived dyes, Environ. Prog. Sustainable Energy 33 (2014) 873–885.

[23] R. Molinari, F. Pirillo, M. Falco, V. Loddo, L. Palmisano, Photocatalytic degradation of dyes by using a membrane reactor, Chem. Eng. Process. 43 (2004) 1103–1114.

[24] I. Vergili, Y. Kaya, U. Sen, Z.B. Gönder, C. Aydiner, Techno-economic analysis of textile dye bath wastewater treatment by integrated membrane processes under the zero liquid discharge approach, Resour. Conserv. Recycl. 58 (2012) 25–35.

[25] B. Mondal, V.C. Srivastava, J.P. Kushwaha, R. Bhatnagar, S. Singh, I.D. Mall, Parametric and multiple response optimization for the electrochemical treatment of textile printing dye-bath effluent, Sep. Purif. Technol. 109 (2013) 135–143.

[26] G.R.P. Malpass, D.W. Miwa, D.A. Mortari, S.A.S. Machado, A.J. Motheo, Decolorisation of real textile waste using electrochemical techniques: Effect of the chloride concentration, Water Res. 41 (2007) 2969–2977.

[27] A.K. Verma, R.R. Dash, P. Bhunia, A review on chemical coagulation/flocculation technologies for removal of colour from textile wastewaters, J. Environ. Manage. 93 (2012) 154–168.

[28] S. Hussain, S. Gul, S. Khan, H. ur Rehman, Retention studies of chromium (VI) from aqueous solution on the surface of a novel carbonaceous material, Arab. J. Geosci. 6 (2012) 4547–4556.

[29] S. Hussain, S. Gul, S. Khan, H. Rehman, M. Ishaq, A. Khan, F.A. Jan, Z. Din, Removal of Cr(VI) from aqueous solution using brick kiln chimney waste as adsorbent, Desalin. Water Treat. 53 (2015) 373–381.

[30] A. Mittal, V. Thakur, J. Mittal, H. Vardhan, Process development for the removal of hazardous anionic azo dye Congo red from wastewater by using hen feather as potential adsorbent, Desalin. Water Treat. 52 (2013) 227–237.

[31] H. Daraei, A. Mittal, M. Noorisepehr, F. Daraei, Kinetic and equilibrium studies of adsorptive removal of phenol onto eggshell waste, Environ. Sci. Pollut. Res. Int. 20 (2013) 4603–4611.

[32] J. Mittal, V. Thakur, A. Mittal, Batch removal of hazardous azo dye Bismark Brown R using waste material hen feather, Ecol. Eng. 60 (2013) 249–253.

[33] J. Mittal, D. Jhare, H. Vardhan, A. Mittal, Utilization of bottom ash as a low-cost sorbent for the removal and recovery of a toxic halogen containing dye eosin yellow, Desalin. Water Treat. 52 (2013) 4508–4519.

[34] G. Sharma, M. Naushad, D. Pathania, A. Mittal, G.E. El-desoky, Modification of *Hibiscus cannabinus* fiber by graft copolymerization: Application for dye removal, Desalin. Water Treat. (2014) 1–8.

[35] R. Jain, P. Sharma, S. Sikarwar, J. Mittal, D. Pathak, Adsorption kinetics and thermodynamics of hazardous

dye Tropaeoline 000 unto Aeroxide Alu C (Nano alumina): A non-carbon adsorbent, Desalin. Water Treat. 52 (2013) 7776–7783.

[36] V.K. Gupta, A. Mittal, L. Krishnan, V. Gajbe, Adsorption kinetics and column operations for the removal and recovery of malachite green from wastewater using bottom ash, Sep. Purif. Technol. 40 (2004) 87–96.

[37] A. Mittal, L. Krishnan, V. Gupta, Removal and recovery of malachite green from wastewater using an agricultural waste material, de-oiled soya, Sep. Purif. Technol. 43 (2005) 125–133.

[38] A. Mittal, Adsorption kinetics of removal of a toxic dye, Malachite Green, from wastewater by using hen feathers, J. Hazard. Mater. 133 (2006) 196–202.

[39] A. Mittal, L. Kurup, Column operations for the removal and recovery of a hazardous dye “acid red—27” from aqueous solutions, using waste rnateria!s—Bottom ash and de-oiled soya, Ecol. Environ. Conserv. 12 (2006) 181–186.

[40] A. Mittal, Removal of the dye, amaranth from waste water using hen feathers as potential adsorbent, J. Environ. Agric. Food Chem. 5 (2006) 1296–1305.

[41] M. Naushad, A. Mittal, M. Rathore, V. Gupta, Ion-exchange kinetic studies for Cd(II), Co(II), Cu(II), and Pb(II) metal ions over a composite cation exchanger, Desalin. Water Treat. (2014) 1–8.

[42] H. Daraei, A. Mittal, M. Noorisepehr, J. Mittal, Separation of chromium from water samples using eggshell powder as a low-cost sorbent: Kinetic and thermodynamic studies, Desalin. Water Treat. 53 (2013) 214–220.

[43] H. Daraei, A. Mittal, J. Mittal, H. Kamali, Optimization of Cr(VI) removal onto biosorbent eggshell membrane: Experimental & theoretical approaches, Desalin. Water Treat. 52 (2013) 1307–1315.

[44] R. Ahmad, R. Kumar, Adsorption studies of hazardous malachite green onto treated ginger waste, J. Environ. Manage. 91 (2010) 1032–1038.

[45] T.S. Anirudhan, P.S. Suchithra, Humic acid-immobilized polymer/bentonite composite as an adsorbent for the removal of copper(II) ions from aqueous solutions and electroplating industry wastewater, J. Ind. Eng. Chem. 16 (2010) 130–139.

[46] M. Ahmaruzzaman, S. Laxmi Gayatri, Batch adsorption of 4-nitrophenol by acid activated jute stick char: Equilibrium, kinetic and thermodynamic studies, Chem. Eng. J. 158 (2010) 173–180.

[47] O. Duman, E. Ayranci, Adsorptive removal of cationic surfactants from aqueous solutions onto high-area activated carbon cloth monitored by *in situ* UV spectroscopy, J. Hazard. Mater. 174 (2010) 359–367.

[48] Y.-S. Ho, Review of second-order models for adsorption systems, J. Hazard. Mater. 136 (2006) 681–689.

[49] S. Noreen, H.N. Bhatti, Fitting of equilibrium and kinetic data for the removal of Novacron Orange P-2R by sugarcane bagasse, J. Ind. Eng. Chem. 20 (2014) 1684–1692.